HIGH-SPEED IMPULSIVE NOISE AND AERODYNAMIC RESULTS FOR RECTANGULAR AND SWEPT ROTOR BLADE TIP TESTS IN S1-MODANE WIND TUNNEL

by C. Polacsek, P. Lafon
Office National d'Etudes et de Recherches Aérospatiales,
BP 72, 92322 Châtillon Cedex, France

Abstract

High-Speed Impulsive (HSI) helicopter rotor noise, performance and local pressure measurements were performed in July-August 1990 in the ONERA S1-Modane wind tunnel fitted with acoustic lining. The acoustic lining improves quality of noise measurements, for the same aerodynamic performance, and makes acoustic averaged signals more workable, especially for HSI noise.

This paper presents acoustic and aerodynamic results obtained by comparing two four-bladed rotors equipped with different sets of blade tip shapes : rectangular (rotor 7A) and sweptback with anhedral (rotor 7AD). The data analysis allows us to compare the aerodynamic performance of the two rotors and to verify that the shock delocalization in the forward direction is decreased with the sweptback parabolic tip blades (7AD).

A gain of 8 dBA on Sound Pressure Level (SPL) is obtained just before delocalization with the rotor 7AD, and the aerodynamic efficiency is improved too. It confirms the interest of the "dihedral concept". Aerodynamic and acoustic results constitute a data base for the validation of computer codes under development.

NOTATIONS

c	:	Blade chord
$(C_d S)_f / (S\sigma)$	:	Propulsive coefficient
C_L/σ	:	Lift coefficient
D	:	Rotor diameter
$M_{\Omega R}$	:	Rotation tip Mach number
M_p	:	Advancing tip Mach number
N	:	Rotation frequency
r	:	Radial distance measured from the rotor hub
R	:	Rotor radius
$T = 1/N$	:	Period of the rotor revolution
μ	:	Advance ratio
σ	:	Solidity of the rectangular blades

ABBREVIATIONS

HSI noise	:	High-Speed Impulsive noise
SPL	:	Sound Pressure Level

I - INTRODUCTION

The geometry of helicopter main-rotor blades is a key parameter for aerodynamic and acoustic rotors performance (Ref. 1). Computer codes therefore have been developed in order to design different blade tip shapes which could improve performance, in particular for high speed (Ref. 2).

As an example, a sweptback parabolic tip with anhedral, designed aerodynamically by ONERA, was chosen to equip the Super Puma Mark II helicopter.

To assess the "dihedral effect", preliminary helicopter rotor tests were performed in the large S1-MA wind tunnel (the test section is 8 meters in diameter) at the Modane-Avrieux ONERA center in August 1988 without acoustic lining and without pressure instrumentation on the blades (Ref. 3).

Following this campaign, aerodynamic and acoustic high-speed tests have been performed in S1-MA in July-August 1990 on pressure instrumented versions of the same rotors, with acoustic lining on the walls of the wind tunnel (Figure 1).

During this campaign, two rotors, 4.2 m in diameter, named 7A and 7AD, are compared. The only difference between them is the blade tip shape : rectangular for the 7A, swept with anhedral for the 7AD. The main objectives of

these tests are :

- To measure the acoustic performance of a four-bladed rotor for two different sets of blade tip shapes.
- To measure the aerodynamic performance and obtain preliminary local blade pressure results for these two rotors.
- To verify if HSI noise, related to shock delocalization, is decreased with the sweptback parabolic tip blades (7AD).
- To constitute a data base for the validation of computer codes under development.

This paper presents the results of aerodynamic and acoustic measurements performed during this campaign. Furthermore, comparison between the two rotors and qualitative correlation between acoustic and aerodynamic results are made.

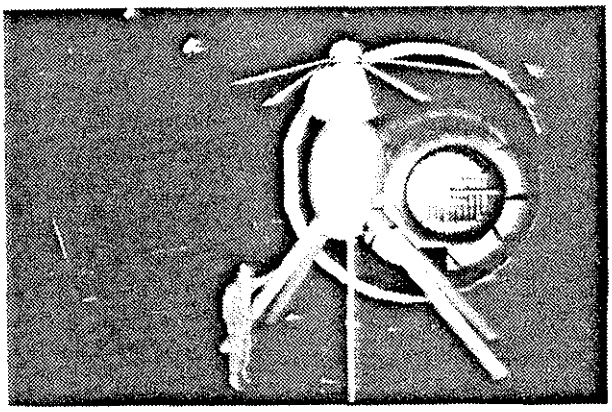

Figure 1 - Helicopter rotor tests in S1-MA wind tunnel with acoustic lining on the walls.

II - EXPERIMENTAL SET-UP, DATA PROCESSING AND TEST PROCEDURE

II.1 - Test Bench

A new test rig (Ref. 3) was built for the S1-MA transonic wind tunnel in order to suppress two main problems : a ground resonance which was observed during an earlier campaign and prohibitive installation time.

The new rotor test rig was qualified in November 1987.

During the 1990-campaign, the maximum airspeed was 115 m/s and the maximum advancing tip Mach number was 0.966.

Rotor characteristics :

The main characteristics of the 4-bladed rotor are the following :

- Basic chord (m) : 0.14
- Radius (m) : 2.1
- Number of blades : 4
- Solidity : 0.085
- Cutout (r/R) : 0.202
- Airfoils :
  - . 0.202 R to 0.75 R : 0A213
  - . 0.9 R to R : 0A209
- Hub offset (m) : 0.075

A complete description of the S1-Modane rotor rig is detailed in Ref. 3.

Blade planforms (Figure 2) :

The blades are equipped with removable tips and two blade tip shapes have been tested :

- rectangular as a reference (rotor 7A),
- sweptback parabolic with anhedral (rotor 7AD).

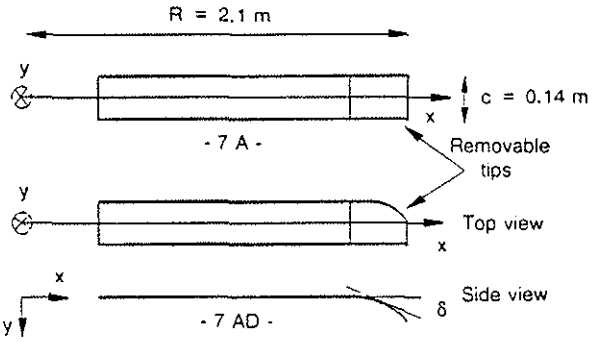

Figure 2 - Blade planforms of the four-bladed rotor

II.2 - Blade Instrumentation and Data Processing for Pressure Measurements

Figure 3 shows the distribution of the absolute unsteady blade pressure transducers. The full instrumentation is composed of 116 transducers :

- 5 spanwise stations with 20 pressure transducers,
- 16 leading edge pressure transducers located at ≃ 3 % chord (upper and lower surface).

This instrumentation is distributed on the four-rotor blades. One blade is also equipped with a radial distribution of strain gages measuring bending and torsion moments along the blade. They will be used to test a Strain Pattern Analysis (SPA) technic. Hot films are also mounted on the blades to study, in particular, flow separation and boundary layer transition.

The results presented in this paper concern preliminary tests performed with acoustic lining (with acoustic measurements as main objective) and only some pressure results obtained for the outboard spanwise station will be considered. This station (r/R = 0.975) is located on the removable tip (Figure 3).

For the unsteady pressure measurements, 128 azimuth are considered for one rotor revolution. At each of these azimuth the measurements are averaged over 30 samples taken for a similar blade azimuth.

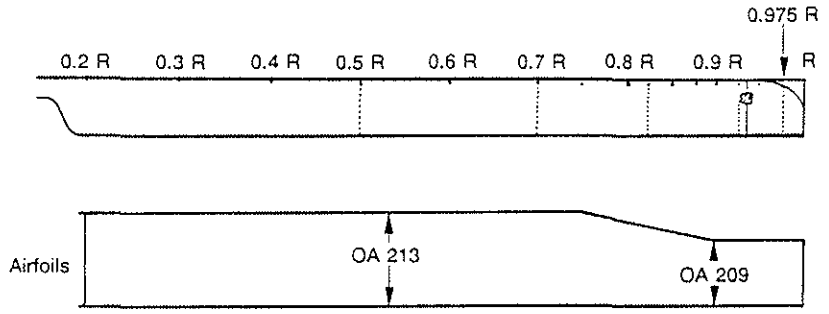

Figure 3 - Blade instrumentation

II.3 - Experimental Set-up and Data Processing for Acoustics

The experimental set-up is shown in Figure 4.

Microphone 4 is the most interesting for HSI noise measurements because it is located in the forward direction, in the rotor plane, where radiation of high-speed noise is maximum. Point P represents the location of a small burst source used as an impulsive noise source in order to characterize remaining acoustic reflections.

Microphones 2, 5, 4, 9, 10 are in the far field (≥ 1.5 D), and are expected to measure the acoustic pressure, approximately decreasing with a 1/r factor. The other microphones measure near-field aerodynamic pressure fluctuations, and do not allow for acoustic extrapolation to the far field.

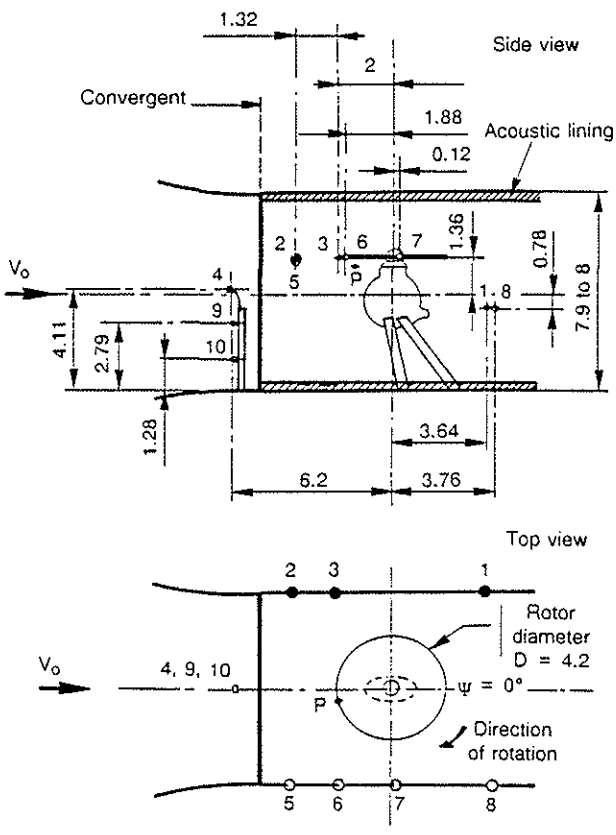

Figure 4 - Experimental set-up of test rig and microphones in the S1-MA wind tunnel *(Dimensions are in meters)*

Data processing :

Measurements only concern harmonic rotor noise, due to the periodic phenomena caused by blade rotation. Therefore, a synchronous rotation analysis allows us to suppress broadband noise and other harmonic noise not generated by the rotor.

Main data processing parameters are :

- N = 16 Hz
- T = 63 ms
- Sampling frequency = 1024 N = 16 kHz.

II.4 - Test procedure

The tests procedure is as follows :

- Imposed conditions for one test configuration :
  - Total lift or lift coefficient C_L/σ (computed with the solidity of the rectangular blades).
  - Propulsive coefficient : $(C_d S)_f / (S \sigma)$ (σ of the rectangular blades).
  - Rotating tip Mach number $M_{\Omega R}$.
  - Advance ratio μ.
- Cyclic control law used :
  - $\theta_{1s} = \beta_{1c}$ (longitudinal cyclic pitch = longitudinal tilt)
  - $\beta_{1s} = 0$ (zero lateral tilt).

The rotor performance is evaluated from the direct measurements made with a six component-balance and a torquemeter.

The S1-Modane wind tunnel is particularly well suited for high advance ratio configurations ($\mu > 0.2$) and for high speed performance and impulsive noise studies.

III - EXPERIMENTAL RESULTS

III.1 - Influence of the Lining on the Aerodynamic and Acoustic Measurements

Performance measurements :

Figure 5 presents the comparative performance of the rotor 7A obtained in the wind tunnel with and without the acoustic lining. The results show that the wall acoustic lining has no effect on the total performance.

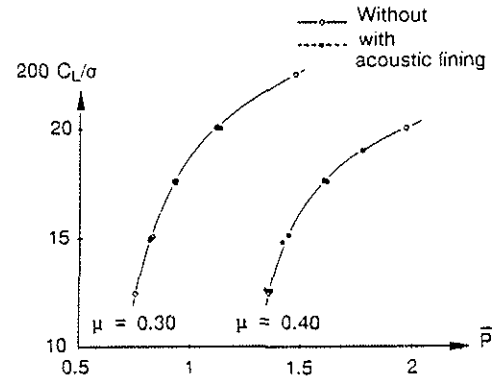

Figure 5 - Comparison with and without acoustic lining : rotor 7A
$(CdS)_f/S\sigma = 0.1$; $M_{\Omega R} = 0.646$;
Control law $\begin{cases} \theta_{1s} = \beta_{1c} \\ \beta_{1s} = 0 \end{cases}$

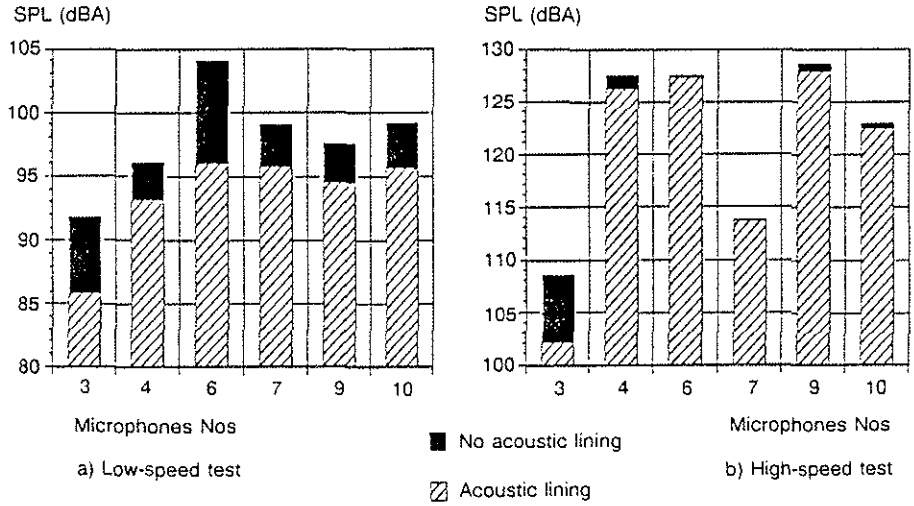

Figure 6 - Comparisons of the sound pressure levels obtained with and without acoustic lining

Acoustic measurements :

Acoustic results are presented in Figure 6, which shows SPL expressed in dBA, scaled to a full-scale Dauphin (12 m in diameter), in low-speed and high-speed conditions, for 6 microphones.

The lining largely reduces the acoustic levels and improves the quality of the time signatures, due to weaker reflections. Typical results are presented in Figure 7 : the lining prevents from the occurrence of a second peak in the averaged time history. The comparison between Figure 7a and Figure 7b shows that the second peak of the time signature observed without lining, not apparent in Figure 7b, is due to wall reflections.

REMARK : In Figure 7a, the averaged time history is presented on two revolutions periods (T = 2/N) instead of one in Figure 7b.

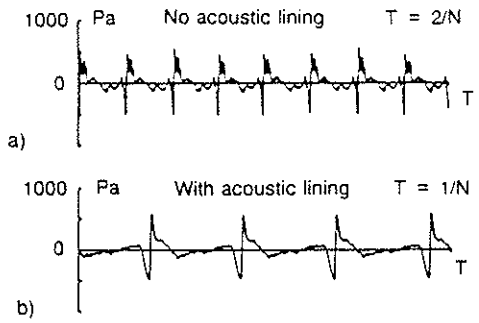

Figure 7 - Example of an averaged time history obtained at high speed (Microphone 4) with and without acoustic lining

III.2 - Comparisons between Rotors 7A and 7AD

III.2.1 - Performance

Figure 8 shows the comparisons between the performance of the rotor 7A (straight blades) and the performance of the rotor 7AD (swept tip with anhedral). These comparisons are presented for the advance ratios μ = 0.2, 0.3, 0.4, 0.45 and 0.5 and for a propulsive force needed to overcome an equivalent fuselage drag coefficient of $(C_d S)_f/S\sigma = 0.1$ (the solidity considered on these figures is the rectangular blade solidity). The improvements in power needed to drive the rotor obtained with the rotor 7AD are between 3 and 6 percents for low and moderate lifts with larger values at high advance ratios. For higher lifts, the difference is smaller.

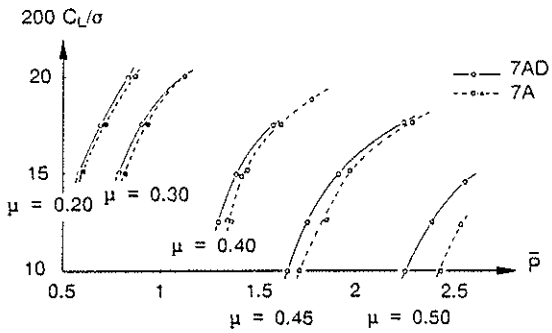

Figure 8 - Comparison rotor 7A/7AD
$(CdS)_f/S\sigma = 0.1$; $M_{\Omega R} = 0.646$;
Control law $\begin{cases} \theta_{1s} = \beta_{1c} \\ \beta_{1s} = 0 \end{cases}$

III.2.2 - Acoustic Results

The aim of these comparisons is to quantify the eventual high-speed noise reduction obtained with 7AD tips.

In particular, the delocalization phenomenon is considered. Delocalization appears when, referencing to the sonic cylinder (Mach = 1), the inner supersonic region is connected to the outer one (Ref. 4).

It is known that the noise changes in nature at the delocalization tip Mach number (function of μ and of the blade geometry), above which a shock radiates from the vicinity of the blade tip to the far field in the upstream direction, causing intense impulsive noise (see also Ref. 5).

Typical results obtained with Microphone 4 are presented in Figure 9 for the rotor 7AD. Delocalization (Figure 9b) is characterized by a steep recompression peak in the acoustic signature associated with an enrichment of the spectrum in higher harmonics, compared to the non delocalizated case (Figure 9a).

Figure 10 presents typical results for the two rotors, respectively at μ = 0.4, Mp = 0.9 (Figure 10a), and μ = 0.45, Mp = 0.933 (Figure 10b). The noise reduction obtained with the rotor 7AD is about 3 to 4 dB compared to the rectangular blades, which corresponds to a decrease of the peak pressure amplitude. This phenomenon is more clearly shown in Figure 11, for the same configurations as in Figure 10.

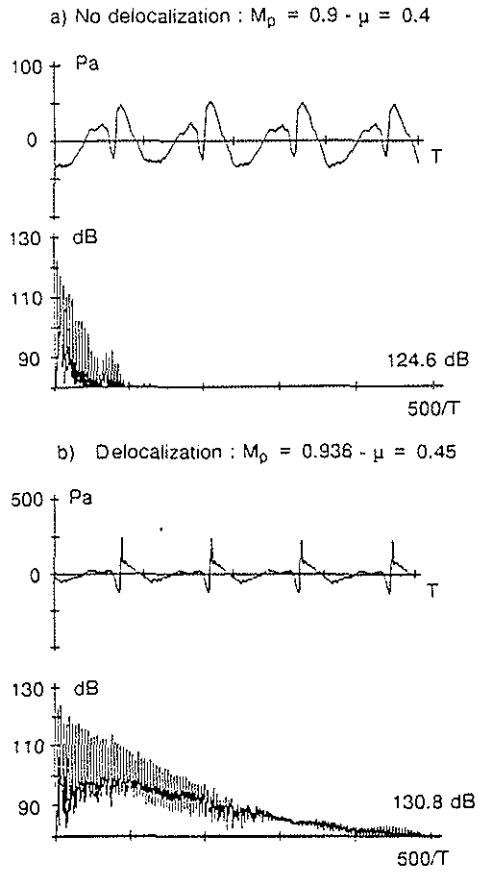

Figure 9 - Typical results : rotor 7AD (Microphone 4)

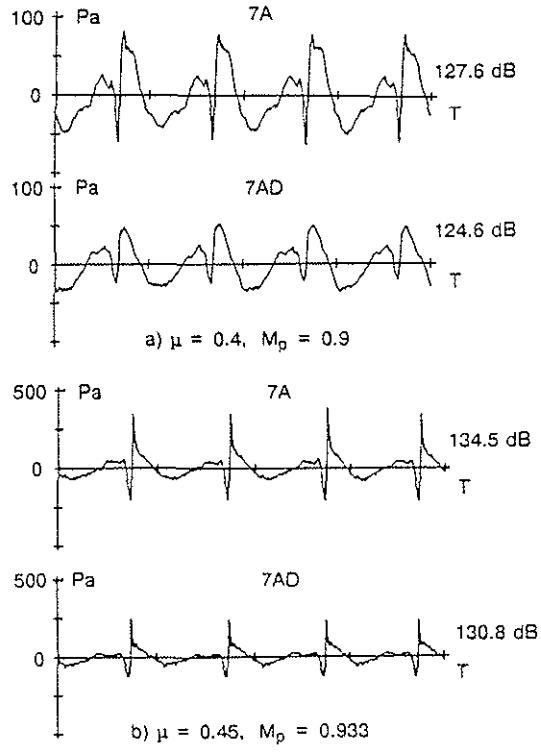

Figure 10 - Comparison between the two rotors under delocalization (Microphone 4)

Here, the time signatures are obtained by an inverse fast Fourier transform of the A-weighted spectrum, in order to remove the low frequency components and to emphasize the impulsive signals. The overall SPL are expressed in unweighted dB in Figure 10, and in dBA in Figure 11.

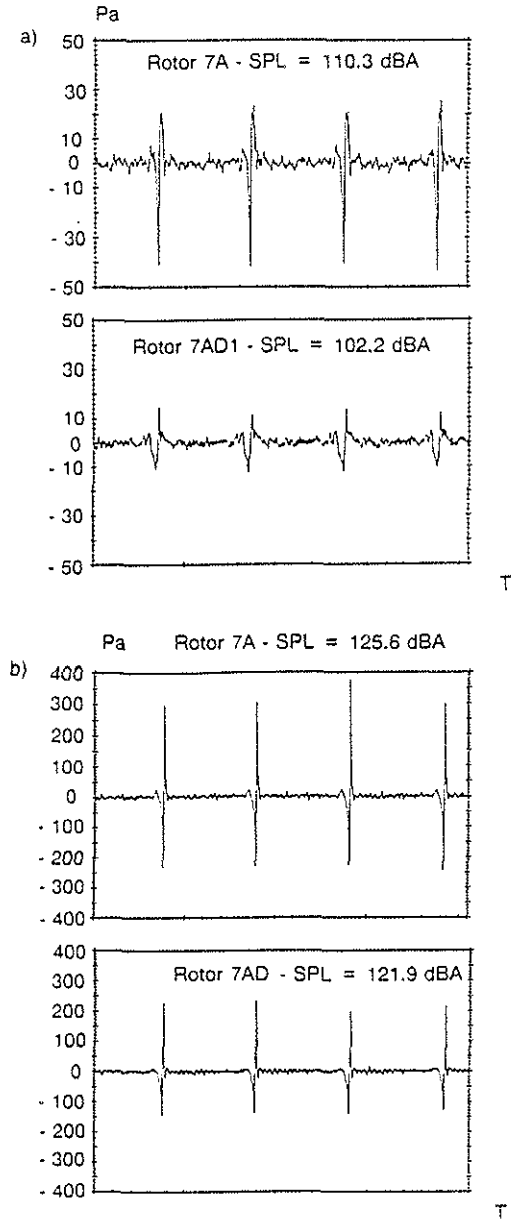

Figure 11 - Comparisons of A-weighted time signatures around delocalization conditions (Microphone 4)

A very large gain (8 dBA) is obtained with the rotor 7AD, at M_p = 0.9. This suggests that the 7AD tip has not yet delocalized unlike 7A, in these conditions. In addition to the beneficial effect of the lining, the A-weighting appears as a simple and efficient way to get a more

realistic result. These results could be used, in a first step for validation of HSI noise codes, at least in the forward direction, in the vicinity of the rotation plane, where noise radiation is maximum.
Parametric variations of the SPL for the two rotors as a function of the advancing-tip Mach number is shown in Figure 12. It gives a good estimation of the speed range in which the rotor 7AD is acoustically more performant than the 7A. The evolutions with and without acoustic lining are similar (respectively Figures 12a and 12b). Measurements in presence of lining provide a larger noise reduction with 7AD in a velocity range slightly reduced.

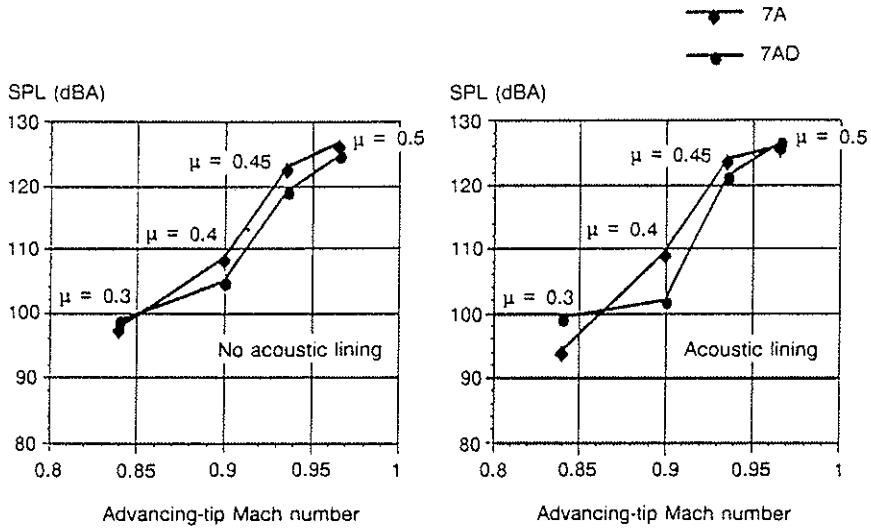

Figure 12 - Comparisons of the sound pressure levels measured with the rotor 7A and 7AD (Microphone 4)

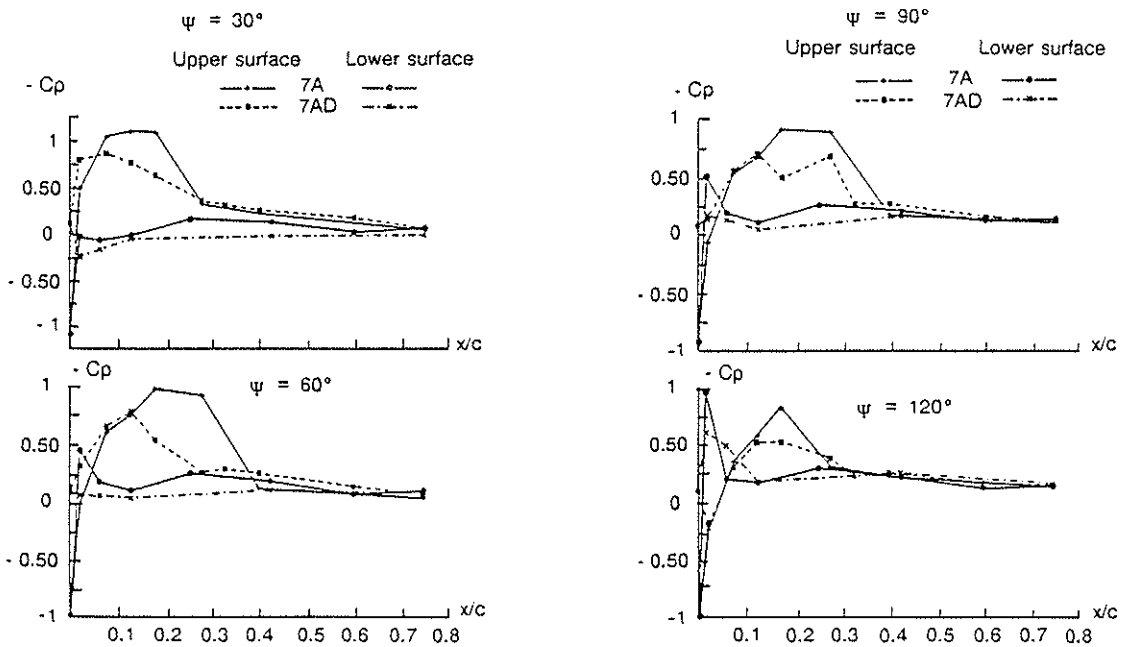

Figure 13 - Comparison rotor 7A/7AD
$C_L/\sigma = 0.1$; $M_{\Omega R} = 0.644$; $(CdS)_f/S\sigma = 0.1$; $r/R = 0.975$; $\mu = 0.3$

III.2.3 - Local Blade Pressure Results

Local pressure distributions are presented for both tips in the spanwise station 0.975 R at azimuthal blade locations 30, 60, 90, 120° in Figure 13. Decrease of the shock waves and transonic flow intensities is noticed on the sweptback parabolic tip with anhedral effect. This effect is the main reason for the noise reduction related to the increase in delocalization Mach number and for the improvement in performance obtained with the rotor 7AD.

The decrease of the intensity of the transonic flows on the advancing blade side obtained with the rotor 7AD is confirmed with the pressure evolutions versus azimuth presented on Figures 14 ($\mu = 0.4$, $C_L/\sigma = 0.06$) and 15 ($\mu = 0.4$, $C_L/\sigma = 0.1$).

A phase shift of the transonic flows towards the second quadrant can be also noticed on the sweptback tip.

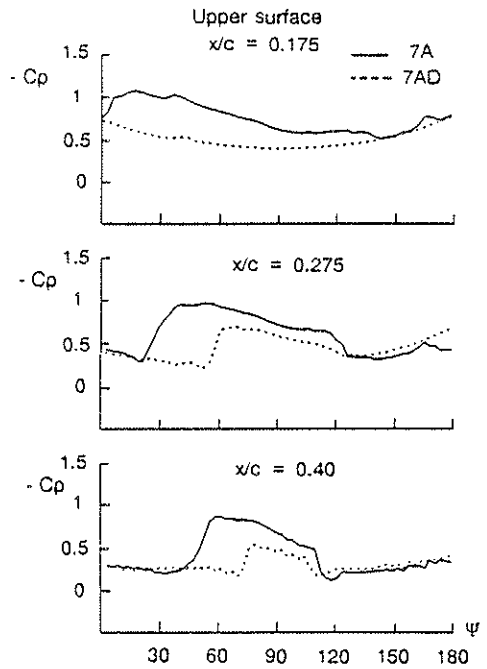

Figure 14 - Comparison rotor 7A/7AD
r/R = 0.975 ; Mu = 0.4 ; $M_{\Omega R}$ = 0.644 ;
C_L/σ = 0.06 ; $(CdS)_f/S\sigma$ = 0.1

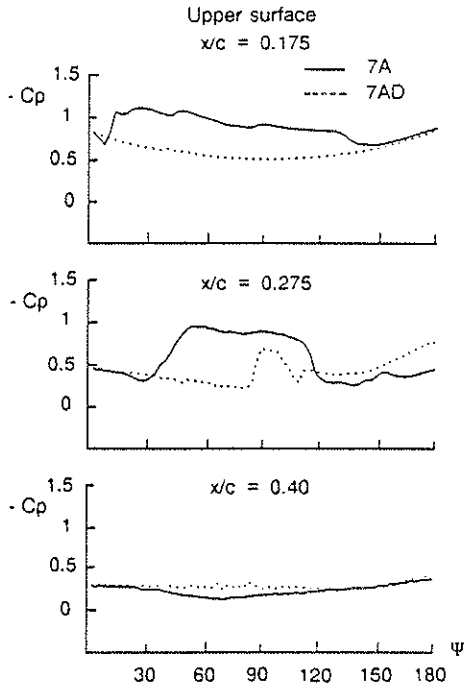

Figure 15 - Comparison rotor 7A/7AD
r/R = 0.975 ; Mu = 0.4 ; $M_{\Omega R}$ = 0.644 ;
C_L/σ = 0.1 ; $(CdS)_f/S\sigma$ = 0.1

IV - CONCLUSION

HSI noise, performance and local blade pressure measurements were performed in July-August 1990 in the ONERA S1-MA wind tunnel fitted with acoustic lining. Two different sets of blade tip shapes : rectangular (rotor 7A) and sweptback parabolic with anhedral (rotor 7AD) have been tested.

Performance comparisons between the two rotors show that the improvement obtained with the rotor 7AD is quite significant compared to the rotor 7A (from 3 to 6 %).

Local pressure measurements indicate clearly a decrease of the shock waves and transonic flow intensities on the sweptback parabolic tip with anhedral effect. This decrease of the transonic flow intensities is the main reason for the noise reduction related to the increase in delocalization Mach number, and for the improvement in performance obtained with the 7AD.

Experiments with the full blade instrumentation are going to be performed and will complete the results already obtained to constitute a data base for the validation of computer codes under development.

REFERENCES

Ref. 1 : A. Desopper, P. Lafon, J.J. Philippe and J. Prieur
"Effect of an Anhedral Sweptback Tip on the Performance of an Helicopter Rotor"
Vertica, Vol. 12, No. 4, 1988, pp. 345-355.

Ref. 2 : J. Prieur
"Calculation of Transonic Rotor Noise Using a Frequency-Domain Formulation"
AIAA Paper 86-1901, 10th Aeroacoustics Conference, Seattle, Washington,
July 1986, and AIAA Journal, Vol. 26, No. 2, February 1988, pp. 156-162.

Ref. 3 : M. Allongue and J.P. Drevet
"New Rotor Test Rig in the Large Modane Wind Tunnel"
Paper No. 98, 15th European Rotorcraft Forum, Amsterdam, September 1989.

Ref. 4 : F.H. Schimtz and Y.H. Yu
"Transonic Rotor Noise Theoretical and Experimental Comparisons"
Paper No. 22, 6th European Rotorcraft and Powered Lift Aircraft Forum, Bristol, England, September 1980, and Vertica, Vol. 5, No. 1, 1981, pp. 55-74.

Ref.5 : J. Prieur
"Experimental Study of High-Speed Impulsive Rotor Noise in a Wind Tunnel"
Paper No. II.9.1, 16th European Rotorcraft Forum, Glasgow, September 1990.